Published in final edited form as:
Biomaterials. 2007 October ; 28(28): 4068–4077.

The effect of actin disrupting agents on contact guidance of human embryonic stem cells

Sharon Gerecht[1,§], **Christopher J. Bettinger**[2,§], **Zhitong Zhang**[3], **Jeffrey Borenstein**[4], **Gordana Vunjak-Novakovic**[5], and **Robert Langer**[1,3,*]

1 *Harvard-M.I.T. Division of Health Sciences and Technology, Massachusetts Institute of Technology, Cambridge, Massachusetts, USA, 02139*

2 *Department of Materials Science and Engineering, Massachusetts Institute of Technology, Cambridge, Massachusetts, USA, 02139*

3 *Department of Chemical Engineering, Massachusetts Institute of Technology, Cambridge, Massachusetts, USA, 02139*

4 *MEMS Technology Group, Charles Stark Draper Laboratory Cambridge, MA, USA 02139*

5 *Department of Biomedical Engineering, Columbia University, New York NY, USA, 10027.*

Abstract

Mammalian cells respond to their substrates by complex changes in gene expression profiles, morphology, proliferation and migration. We report that substrate nanotopography alters morpohology and proliferation of human embryonic stem cells (hESCs). Fibronectin-coated poly(dimethyl siloxane) substrates with line-grating (600 nm ridges with 600 nm spacing and 600 +/− 150 nm feature height) induced hESC alignment and elongation, mediated the organization of cytoskeletal components including actin, vimentin, and α-tubulin, and reduced proliferation. Spatial polarization of gamma tubulin complexes was also observed in response to nanotopography. Furthermore, the addition of actin disrupting agents attenuated the alignment and proliferative effects of nanotopography. These findings further demonstrate the importance of interplay between cytoskeleton and substrate interactions as a key modulator of morphological and proliferative cellular response in hESCs on nanotopography.

Introduction

In vivo cellular microenvironments are immobilized within tissue, and consist of diverse extracellular matrix (ECM) proteins that present biophysical cues to the cells via their rich three-dimensional surface topography [1]. The topographic features within basement membranes are on sub-micron length-scales [2]. Individual cells integrate the external cues that arise from their environment and dictate genotypic profiling. Importantly, it is not only the milieu of soluble, diffusible factors, but also the adhesive, mechanical interactions with scaffolding materials that drive the different states and functions of a cell, including gene

* To whom reprint requests should be addressed at: Department of Chemical Engineering, E25-342 Massachusetts Institute of Technology, 77 Massachusetts Avenue, Cambridge, MA 02139. E-mail: rlanger@mit.edu..
§Authors contributed equally to this work

expression, adhesion, migration, proliferation, and differentiation [3–5]. For the binding interactions between the cells and surfaces, it has become increasingly evident that cells are influenced by spatial domains, structural compositions, and mechanical forces at the micro- and nano-scale [6]. Cells use transmembrane actin–integrin adhesion complexes as mechanosensors to probe the rigidity of the extracellular environment, mediate adhesion, trigger signaling, and remodel the ECM [7].

This has led to the widely tested hypothesis that cellular structure and function can be influenced by substrates containing with micron and sub-micron scale topography [8]. Cellular responses to synthetic micro- and nanofabricated substrates [9] via contact guidance [10] has been observed in a variety of mature cell types [11] including, but not limited to epithelial cells [12–14], fibroblasts [15–18], oligodendrocytes [19], astrocytes [19], and endothelial cells [20]. In addition to changes in gross morphology and migration, contact guidance induced up regulation of fibronectin mRNA in human fibroblasts [21], increased adhesion of epithelial cells [13], and increased mineralization and alkaline phosphatase activity in rat bone marrow cells [22].

Human embryonic stem cells (hESCs) have a capability to differentiate into derivatives of all three primary germ layers, both *in vitro* and *in vivo* [23]. Human ESCs differentiation *in vitro* follows temporal patterns that recapitulate early embryogenesis in many ways [24]. The *in situ* environment of a developing blastocyst contains a complex ECM network, forming a micro-environment that has ability to affect cell behavior. ESCs are known to respond to the chemical and mechanical constitution of the ECM through lineage-specific differentiation for example. In this report, we describe the morphological and proliferation responses of hESCs to synthetic nanotopography. Furthermore, we studied the contact guidance responses of hESCs in the presence of actin disrupting agents (ADAs).

We hypothesized that the nanotopography of the substrate can be used to control morphology and proliferation of hESCs via *in vitro* contact guidance responses. Utilizing substrates with nanometer-scale line grating features, we examined the effect of contact guidance of hESCs on cell cytoskeleton organization and proliferation. In addition to gross morphological changes including elongation and alignment of cells with the substrate features, spatial polarization of gamma-tubulin complexes was also observed in cells cultured on nanotopographic substrates. Furthermore, culturing hESCs in the presence of ADAs further demonstrated that cytoskeleton remodeling through actin polymerization is critical in the manifestation of morphological and proliferative aspects of hESCs cultured on nanotopography. To our knowledge, this is the first study to examine and characterize the contact guidance response of hESCs to linear nanotopography in the presence of soluble factors that are able to supercede effects for substrate signaling alone. The identification of downstream effectors of the contact guidance response in hESCs could lead to subsequent investigations to implicate upstream signaling pathways.

Materials and Methods

Fabrication and Preparation of Nanotopographic Substrates

Traditional photolithographic techniques were used to fabricate silicon masters with line-grating geometries with target dimensions of 1200 +/− 200 nm periodicity (600 nm ridges with 600 nm spacing) and 600 +/− 150 nm feature height (MEMS Exchange, Reston, VA). Briefly, 100 mm silicon wafers were coated with Shipley SPR220-3 photoresist, exposed using a GCA AS200 stepper, and post-baked. Wafers were etched using a silicon ICP etch process using SF_6/Argon in a VLR-700. Silicon wafers were then plasma ashed and cleaned for preparation in replica-molding. Silicon masters were used to replica-mold substrates with linear nanotopographic features using poly(di-methylsiloxane) (PDMS, Dow Sylgard 184, Essex Chemical, Clifton, NJ), which was chosen for ease of fabrication and optical clarity to facilitate

characterization. Due to the hydrophobic nature of PDMS, which typically leads to low adhesion of cells to surfaces, fibronectin was adsorbed onto the surface to promote adhesion and attachment of hESCs. Briefly, substrates were plasma cleaned (PDC-001, Harrick Scientific Co) for 300 sec at approximately 80 W RF power with atmospheric gas at pressures between 200 and 500 mTorr. A 2.5 μg/mL solution of fibronectin in PBS (Invitrogen Corporation, Carlsbad, CA) was immediately adsorbed onto the surface, which was incubated for 3 h at 37 °C and 95% humidity. When applied to PDMS substrates, this procedure resulted in fibronectin film thickness of approximately 100 nm in previous studies [25,26]. This suggests that the resulting fibronectin film will not "washout" the nanoscale topography of the substrate.

Human embryonic stem cells culture

Non-differentiating hESCs (lines H9 and H13, WiCell Research Institute, Madison, WI; p19-40) were grown on inactivated mouse embryonic fibroblasts (MEF) in growth medium consisting of 80% KnockOut DMEM, supplemented with 20% KnockOut Serum Replacement, 4 ng/ml basic Fibroblast Growth Factor, 1 mM L-glutamine, 0.1 mM β–mercaptoethanol, 1% non-essential amino acid stock (Invitrogen Corporation, Carlsbad, CA). hESCs were passaged every 4 to 6 d using 1 mg/ml type IV collagenase (Invitrogen Corporation, Carlsbad, CA). For individual cell suspension (i.e. cultured on nanotopographic and flat substrates), hESCs were digested with EDTA 5 mM in PBS, supplemented with 1% (v/v) FBS (HyClone, Logan, UT), and separated into individual cell suspension using a 40-μm mesh strainer (Becton Dickinson –Falcon, San Jose, CA). Undifferentiated hES individual cell suspensions were plated on type-IV collagen-coated six-well dishes (Becton Dickinson, Franklin Lakes, NJ). For contact guidance studies, the cells were seeded on substrates at densities of approximately 10,000 cells per cm^2 in a differentiation medium composed of alpha-MEM medium (Invitrogen Corporation, Carlsbad, CA) supplemented with 10% FBS (HyClone, Logan, UT) and 0.1 mM β-mercaptoethanol (Invitrogen Corporation, Carlsbad, CA).

Inhibitor preparations

For pathways studies, cells were cultured in media with the following respective concentrations of inhibitors in solvents (Sigma, St. Louis, MO) listed as noted: 1 μg/mL cytochalasin D in DMSO, 6.25 μM Latrunculin A (EMD Biosciences, San Diego, CA) in DMSO, 8 μM Latrunculin B (EMD Biosciences, San Diego, CA) dissolved in DMSO. Media was charged with fresh inhibitors during daily exchange and the final concentrations of all solvents were kept below 0.25% (v/v).

Proliferation assays

Cell metabolism was evaluated by the XTT kit (Sigma, St. Louis MO) according to the manufacturer's instructions. Human ESCs were incubated for 4 h in medium containing 20% (v/v) XTT solution. For analysis, triplicates of 150 μl of the medium were removed, placed in a 96-plate well and read in a microplate reader at 450 and 690 nm. Proliferating cells were examined via BrdU incorporation. BrdU staining kit (Invitrogen Corporation, Carlsbad, CA) was used *in situ*, according to manufacturer's instructions. Briefly, cells were incubated with BrdU labeling reagent (1:100) for 24 h, washed several times with PBS (Invitrogen Corporation, Carlsbad, CA), and fixed with 70% ethanol for 30 minutes at 4 °C. A standard staining procedure, provided by the manufacturer, was performed and cells were examined and manually characterized using an inverted light microscope (Zeiss, Germany).

Immunofluorescence of cytoskeleton, focal adhesions, and gamma-tubulin complexes

Human ESCs were fixed *in situ* with accustain (Sigma, St Louis, MO) for 20–25 min at room temperature. After blocking with 5% FBS, cells were stained with one of the following primary

antibodies: anti human alpha smooth muscle actin (SMA; 1:50), anti human calponin, (1:50), anti human vimentin (1:20; all from Dako, CA), anti human vinculin (1:100; Chemicon Temecula, CA), anti human alpha-tubulin (1:20; Sigma, St. Louis, MO), anti phosphorylated myosin light chain (1:50; Cell Signaling), and anti human gamma-tubulin (1:100; Abcam, Cambridge, MA). Cells were then rinsed three times with PBS (Invitrogen corporation, Carlsbad, CA) and incubated for 30 min with suitable Cy3-conjugated (Sigma, St Louis, MO) secondary antibody. Samples were then counterstained with DAPI (1:200; Sigma, St Louis, MO) for 5 min. Cells were imaged using either fluorescence microscopy (Zeiss, Germany) or DeltaVision RT Deconvolution Microscopy (Applied Precision, WA, USA). Exposure times were kept constant across micrographs only when making qualitative comparisons.

Cell morphology imaging and characterization

The transparent PDMS substrates allow for the direct measurement of cell alignment angle using an inverted light microscope (Zeiss, Germany). SEM and phase micrographs of cells using a 10X objective lens were used to characterize morphological parameters for each sample analyzed. The circularity [27] and alignment angle of the cell were calculated manually using perimeter and area measurements by using Axiovision software (Zeiss, Germany). Digital zoom was used to increase the magnification and, in turn, increase the accuracy of the measurements. Alignment angle was calculated by fitting an ellipse to the cell body, measuring the relative normalized angle between the major axis and the feature orientation. The cell areas and perimeters were measured using Axiovision measurement software and were used to calculate the circularity using the following formula:

$$C=\frac{4\pi A}{P^2} \qquad \text{(Eqn. 1)}$$

where A is the projected area of the cell and P is the perimeter of the cell. Circularity was used as a metric of cell elongation; average angle was used as an index cell alignment (Supplementary Fig 1A–B). SEM was also used to assess three-dimensional morphology. Characterization of polarized gamma tubulin complexes (GTCs) was performed by calculating the angle made between the longitudinal axis of the nucleus and the line containing the GTC of interest to the center of the nucleus (Supplementary Fig 1C).

Scanning Electron Microscopy

Cells were fixed with accustain formalin-free fixative (Sigma, St Louis, MO) for 20 min at room temperature, washed three times with DPBS, and post-fixed with 1% (w/w) OsO4 in water for 20 min. A graded ethanol series was implemented for dehydration of the cells (25%, 50%, 75%, and 90%, 100% v/v ethanol in ddH_20), 5 min per step. The samples were then immersed for 10 min in 100% ethanol followed by HMDS (Sigma), and allowed to air dry at room temperature for 24 h prior to imaging. Samples were sputter-coated using a Cressington 108 Auto sputter coater (Cressington Scientific Instruments Inc, Cranberry Twp, PA). Scanning electron micrographs were taken using a Hitachi S-3500N at 5kV.

Statistics

All measurements of the cell alignment, circularity, SEM imaging, proliferation, and plating density were performed in triplicate samples across two independent experiments (n = 6). Morphological observations were based on the sampling over at least n = 100 cells per population with a minimum of three cell populations per data point. GTC orientations were calculated from at least 150 total complexes per data point. XTT metabolism assays were performed in triplicate samples (n = 3) with triplicate readings for each data point. One-tailed student's t-tests with unequal variances were performed to determine statistical significance, where appropriate (Microsoft Excel, Redmond, WA). Parametric one-way and two-way ANOVA tests were also performed where appropriate (GraphPad Prism 4.02, GraphPad

Software, San Diego, CA). Bonferroni's multiple comparison post-tests were used to determine significance between specific treatments. All graphical data is reported as mean +/− s.d. Significance levels were set at * $p < 0.05$, ** $p < 0.01$, and *** $p < 0.001$.

Results

Human ESC response to linear substrate nanotopography

PDMS films were established with high fidelity of the feature geometry and dimensions that were verified through SEM (Supplementary Fig 2). Single-cell suspensions of hESCs cultured on nanotopographic substrates responded to linear nanotopography by increased alignment and elongation (Fig 1A), as measured by reduced average angle of alignment and circularity (Fig 1B). Due to the hydrophobic nature of PDMS, a low frequency of hESC attachment on unmodified PDMS substrates was observed. Less than 50% of cells attached to unmodified PDMS when compared to fibronectin-coated surfaces as determined by cell density, although alignment and elongation, fingerprints of the contact guidance response, were observed (data not shown). Therefore, subsequent studies were performed using fibronectin-coated PDMS substrates. Human ESCs cultured on nanotopographic substrates exhibited reduced projected cell areas (Fig 1C) and reduced proliferation, as measured by cell growth kinetics (Fig 1D). Reduced proliferation was also observed at 24 h and 48 h timepoints via BrdU assay (* $p < 0.05$) as assessed by two-way ANOVA ((Fig 1E–F).

Contact guidance induces cytoskeletal organization

Cellular responses to nanotopography including alignment, elongation, and organization of cytoskeleton were observed on substrates with nanotopography. Linear nanotopographic substrates organized cytoskeletal components, which was evident through differences in morphology, and cytoskeletal filaments organization and alignment in the same axis as the grid-lines including α-SMA, vimentin, an intermediate filament which forms part of the cytoskeleton, as well as, α-tubulin, and calponin (Fig 2). Cell alignment was further verified by SEM micrographs (Fig 2), deconvolution fluorescent microscopy (Fig 3), and reconstructed videos of z-stack micrographs (Supplementary Videos 1–3) in hESCs after 24 h.

Polarization of gamma-tubulin complexes (GTCs)

GTCs were present in hESCs at the frequency of approximately 2.98 GTCs per cell. GTCs present in hESCs cultured on flat substrates exhibit a random radial distribution with respect to the longitudinal axis of the nucleus when compared to cells cultured on nanotopographic substrates (Fig 4). The average normalized angle of GTCs in hESCs cultured on flat and nanotopographic substrates, was observed to be 40.68 +/− 25.42 degrees and 28.42 +/− 24.72 degrees (mean +/− s.d.), respectively (* $p < 0.05$).

Actin disrupting agents attenuates contact guidance response

To further understand the phenomena of topographic-induced alignment and elongation of hESCs, we examined the effect of two actin disrupting agents (ADAs) on cytoskeleton reorganization and proliferative states; cytochalasin D and latrunculin B (herein also referred to as cyto D and latr B, respectively). The effect of latrunculin A, another actin disrupting agent, was studied. However, poor cell attachment was observed, which prohibited further in-depth study (data not shown). Latr B possesses higher specificity in inhibiting actin polymerization and microfilament-mediated processes. The addition of cyto D and latr B independently reduced the projected area of hESCs cultured on both flat and nanotopographic substrates (Supplementary Fig 3). Cells cultured on nanotopographic substrates in the presence of ADAs lost cytoskeleton organization in a variety of cytoskeletal proteins including α-smooth muscle actin, α-tubulin, vimentin, and calponin (Fig 5). Human ESCs cultured with soluble

ADAs also exhibited a more rounded three-dimensional morphology as indicated by SEM images (Fig 5). Furthermore, the addition of cyto D and latr B to the medium attenuated the contact guidance response by suppressing elongation as measured by circularity, and alignment as measured by the angle of alignment (Fig 6A). The alignment angle was significantly increased in hESCs cultured on nantopographic substrates in the presence of both cyto D and latr B as determined by one-way ANOVA with Bonferroni post-tests (*** $p < 0.001$ and ** $p < 0.01$ for cyto D and latr B, respectively). In general, the addition of ADAs reduced the project surface area and increased circularity on both nanotopographic and flat substrates.

Proliferation rates were also increased in the presence of these agents as demonstrated by increased growth kinetics as measured by cell densities (Fig 6B), which resulted in colonies of rapidly proliferating cells. This observation was corroborated with increased BrdU uptake of cells in the presence of cyto D and latr B at 24 h (*** $p < 0.001$) as determined by one-way ANOVA (Fig 6C). The metabolic activity of the cells was increased in the presence of cyto D (**Fig 6Di**) and latr B (**Fig 6Dii**) alike at 24 h, as measured by XTT cleavage assay. This increase in proliferation and metabolic activity upon the addition of ADAs was observed across both nanotopographic and flat substrates (Supplementary Fig 4). Consequently, the observed reduction in proliferation of hESCs cultured on nanotopographic versus flat substrates is lost in the presence of actin-disrupting agents. The statistical significance of differential BrdU uptake of cells cultured on nanotopographic versus flat substrates is lost in the presence of ADAs (* $p < 0.05$ without ADAs; $p = 0.64$ with ADAs).

Discussion

Our objective was to characterize the *in vitro* contact guidance response of hESCs to ordered substrate nanotopography. Of specific interest was the assessment of gross morphology, alignment, proliferation, and cytoskeleton organization. The hierarchal preference of signaling through substrate chemical patterning versus substrate topography has been studied in various cell types by others. However, we were interested in exploring the coupled effects of soluble factors present in culture medium and nanotopographic cues provided by the substrate.

There have been numerous studies that document contact guidance in mammalian cells using microfabricated substrates with a variety of feature sizes and geometries [11–19]. In this study, the motivation for using a line-grating with 600 nm as a feature size for our subsequent nanotopographic studies was two-fold: 1) Features should be large enough allow fibronectin coating absorbance while maintaining feature fidelity; 2) Features should be small enough to prevent morphological alteration by spatial confinement. The morphological alterations and cytoskeleton protein organization induced by nanotopography in hESCs is in concert with subsequent observations in other mature cell types. Furthermore, we observed that the contact guidance response of hESCs to surface nanotopography includes a significant reduction in proliferation when compared to flat substrates, which is in concert with similar experiments involving mammalian cells including SMCs [28]. The contact guidance response also manifests itself through the organization of cytoskeleton proteins including α-SMA, α-tubulin, vimentin, and calponin. These cytoskeleton proteins became unequivocally oriented in the direction of the grid lines in cells cultured on nanotopographic substrates. The structural bias of cytoskeleton proteins led to the investigation of the possible alignment of microtubule organization centers as well. Microtubules are known to play a critical and active role in governing cytoskeleton function. Gamma-tubulin complexes (GTCs) have been implicated as the initiators of microtubule assembly through the formation of such structures as microtubule organization centers (MTOCs) [29]. The spatial polarization of GTCs induced by nanotopography in hESCs observed in this study suggests that morphological manifestations of the contact guidance response may originate at these localized regions of microtubule formation. The spatial polarization of well-defined MTOCs containing gamma-tubulin has

been previously studied in SMCs on nanotopography in response to wound healing [28] and the presence of gamma-tubulin complexes have also been studied in P19 embryonic carcinoma cells [30].

The assembly of filamentous actin was hypothesized to play a direct role in controlling cytoskeletal and morphological aspects of the contact guidance response in hESCs. Therefore, we investigated the effect of the ADAs cyto D and latr B on gross morphology and the organization of cytoskeleton proteins. Previous studies also reported that cyto D caused observable changes in cellular morphology, with the rounding of the cell body and reduced spreading in mouse mesenchymal stem cells [31,32]. We observed morphological changes including reduction of cell area and organization of cytoskeleton proteins in hESCs cultured on nanotopographic substrates in the presence of ADAs. The observed reduction in cell alignment on nanotopographic substrates may be linked to the impaired ability of the cell to detect and respond to topographic cues presented by the substrate. Furthermore, the cell density, proliferation, and metabolic activity were all subsequently increased, in nanotopographic substrates cultures treated with cyto D or with latr B. This observation has been made in mammalian cells: namely that precluding cytoskeleton organization via inhibition of filamentous actin polymerization suggests a link between cytoskeleton dynamics and proliferation [33,34].

While cyto D and latr B impact cell spreading and proliferation of hESCs cultured on flat substrates as measured by reduced cell area (Supplementary Fig 3) and increased circularity (Supplementary Fig 4A), it was found that disrupting cytoskeleton remodeling activity through the additions of ADAs leads to a loss of the differential morphological and proliferative specificity of hESCs cultured on nanotopographic (Fig 5) versus flat substrates (Supplementary Fig 4A–D). This suggests that the reduced proliferation component of the contact guidance response may be linked to the organization of the cytoskeleton. Furthermore, this cytoskeleton-linked effect of contact guidance on proliferation can be overcome by chemical signaling through soluble factors. It thus appears that there is a link between cytoskeleton function and proliferation that may explain the reduced proliferation of mature cells cultured on nanotopographic surfaces and that this effect can be altered by soluble factors.

CONCLUSIONS

From this work, and studies performed in other laboratories [7,35,36], it is being established that the cytoskeleton is an active organelle with vital cellular function. Human ESCs respond to nanoscale substrate topography in a similar manner as other terminally differentiated mammalian cells, including elongation and alignment, reduced proliferation, and the organization and polarization of cytoskeleton proteins. The cytoskeleton plays an important role in the morphological and proliferative responses to contact guidance cues. However, characteristic morphological and proliferation behavior induced by the contact guidance response can be superceded by soluble factors that directly interact with structural components of cell including actin-based stress fibers.

Supplementary Material

Refer to Web version on PubMed Central for supplementary material.

Acknowledgements

The authors would like to acknowledge the following: Dr. Eliza Vasile from the Center for Cancer Research, Microscopy and Imaging Core Facility at MIT for assistance with imagine and deconvolution microscopy, the Juvenile Diabetes Research Foundation (fellowship to S. G-N), the MEMS Technology Group at the Draper Laboratory for direct funding for CJB and use of facilities; funding provided through DL-H-550154; NIH grants R01-DE-013023-06,

P41 EB002520-01A1 and 1R01HL076485-01A2. The content of this paper does not necessarily reflect the position or the policy of the government, and no official endorsement should be inferred.

References

1. Timpl R. Macromolecular organization of basement membranes. Curr Opin Cell Biol 1996;8:618–24. [PubMed: 8939648]
2. Abrams GA, Schaus SS, Goodman SL, Nealey PF, Murphy CJ. Nanoscale topography of the corneal epithelial basement membrane and Descemet's membrane of the human. Cornea 2000;19:57–64. [PubMed: 10632010]
3. Chen CS, Tan J, Tien J. Mechhanotransduction at cell-matrix and cell-cell contacts. Annu Rev Biomed Eng 2004;6:275–302. [PubMed: 15255771]
4. McBeath R, Pirone DM, Nelson CM, Bhadriraju K, Chen CS. Cell Shape, Cytoskeletal Tension, and RhoA Regulate Stem Cell Lineage Commitment. Dev Cell 2004;6:483–95. [PubMed: 15068789]
5. Watt FM, Jordan PW, O'Neill CH. Cell shape controls terminal differentiation of human epidermal keratinocytes. Proc Natl Acad Sci USA 1988;85:5576–80. [PubMed: 2456572]
6. Sniadecki NJ, Desai RA, Ruiz S, Chen SC. Nanotechnology for cell-substrate interactions. Ann Biomed Eng 2006;34(1):59–74. [PubMed: 16525764]
7. Geiger B, Bershadsky A, Pankov R, Yamada KM. Transmembrane crosstalk between the extracellular matrix--cytoskeleton crosstalk. Nat Rev Mol Cell Biol 2001;2(11):793–805. [PubMed: 11715046]
8. Curtis A, Wilkinson C. Topographical control of cells. Biomaterials 1997;18(24):1573–81. [PubMed: 9613804]
9. Curtis A, Wilkinson C. Nanotechniques and approaches in biotechnology. Trends Biotechnol 2001;19 (3):97–101. [PubMed: 11179802]
10. Weiss P. Experiments on cell and axon orientation in vitro: the role of colloidal exudates in tissue organization. J Exp Zool 1945;100:353–86.
11. Flemming RG, Murphy CJ, Abrams GA, Goodman SL, Nealey PF. Effects of synthetic micro- and nano-structured surfaces on cell behavior. Biomaterials 1999;20:573–88. [PubMed: 10213360]
12. Teixeira AI, Abrams GA, Bertics PJ, Murphy CJ, Nealey PF. Epithelial contact guidance on well-defined micro- and nanostructured substrates. J Cell Sci 2003;116:1881–92. [PubMed: 12692189]
13. Karuri NW, Liliensiek S, Teixeira AI, Abrams G, Campbell S, Nealey PF, et al. Biological length scale topography enhances cellsubstratum adhesion of human corneal epithelial cells. J Cell Sci 2004;117:3153–64. [PubMed: 15226393]
14. Brunette DM. Spreading and orientation of epithelial cells on grooved substrata. Exp Cell Res 1986;167:203–17. [PubMed: 3758202]
15. Walboomers XF, Monaghan W, Curtis A, Jansen JA. Attachment of fibroblasts on smooth and microgrooved polystyrene. J Biomed Mater Res 1999;46:212–20. [PubMed: 10379999]
16. Walboomers XF, Croes H, Gensel LA, Jansen JA. Contact guidance of rat fibroblasts on various implant materials. J Biomed Mater Res 1999;47:204–12. [PubMed: 10449631]
17. Brunette DM. Fibroblasts on micromachined substrata orient hierarchically to grooves of different dimensions. Exp Cell Res 1986;164:11–26. [PubMed: 3956588]
18. Braber, ETd; Ruijter, JEd; Smits, H.; Ginsel, LA.; Recum, AFv; Jansen, JA. Quantitative analysis of fibroblast morphology on microgrooved surfaces with various groove and ridge dimensions. Biomaterials 1996;17:2037–44. [PubMed: 8902235]
19. Webb A, Clark P, Skepper J, Compston A, Wood A. Guidance of oligodendrocytes and their progenitors by substratum topography. J Cell Sci 1995;108:2747–60. [PubMed: 7593316]
20. Bettinger CJ, Orrick B, Misra A, Langer R, Borenstein JT. Microfabrication of poly(glycerol-sebacate) for contact guidance applications. Biomaterials 2006;27:2558–65. [PubMed: 16386300]
21. Chou L, Firth JD, Uitto VJ, Brunette DM. Substratum surface topography alters cell shape and regulates fibronectin mRNA level, mRNA stability, secretion and assembly in human fibroblasts. J Cell Sci 1995;108:1563–73. [PubMed: 7615675]
22. Matsuzaka K, Walboomers F, Ruijter Ad, Jansen JA. Effect of microgrooved poly-l-lactic (PLA) surfaces on proliferation, cytoskeletal organization, and mineralized matrix formation of rat bone marrow cells. Clin Oral Impan Res 2000;11(4):325–33.

23. Thomson JA, Itskovitz-Eldor J, Shapiro SS, Waknitz MA, Swiergiel JJ, Marshall VS, et al. Science 1998;282:1145–7. [PubMed: 9804556]
24. Itskovitz-Eldor J, Schuldiner M, Karsenti D, Eden A, Yanuka O, Amit M, et al. Differentiation of human embryonic stem cells into embryoid bodies compromising the three embryonic germ layers. Mol Med 2000;6:88–95. [PubMed: 10859025]
25. Toworfe GK, Composto RJ, Adams CS, Shapiro IM, Ducheyne P. Effect of surface activated poly (dimethylsiloxane) on fibronectin adsorption and cell function. Mat Res Soc Symp Proc 2004;EXS-1:F7.8.1–F7.8.5.
26. Toworfe GK, Composto RJ, Adams CS, Shapiro IM, Ducheyne P. Fibronectin adsorption on surface-activated poly(dimethylsiloxane) and its effect on cellular function. J Biomed Mater Res 2004;71A: 449–61.
27. Thurston G, Jaggi B, Palcic B. Measurement of cell motility and morphology with an automated microscope system. Cytometry 1988;9(5):411–7. [PubMed: 3180942]
28. Yim EKF, Reano RM, Pang SW, Yee AF, Chen CS, Leong KW. Nanopattern-induced changes in morphology and motility of smooth muscle cells. Biomaterials. 2005in press
29. Schiebel E. Gamma-tubulin complexes: binding to the centrosome, regulation and microtubule nucleation. Curr Opin Cell Biol 2000;12:113–8. [PubMed: 10679351]
30. Kukharskyy V, Sulimenko V, Macurek L, Sulimenko T, Draberova E, Draber P. Complexes of gamma-tubulin with nonreceptor protein tyrosine kinases Src and Fyn in differentiating P19 embryonal carcinoma cells. Exp Cell Res 2004;298:218–28. [PubMed: 15242776]
31. Smith ER, Smedberg JL, Rula ME, Xu XX. Regulation of Ras-MAPK pathway mitogenic activity by restricting nuclear entry of activated MAPK in endoderm differentiation of embryonic carcinoma and stem cells. J Cell Biol 2004;164(5):689–99. [PubMed: 14981092]
32. Hussain MA, Yourek G, Mao JJ. Nanomechanobiology of cytoskeletal changes in mesenchymal stem cells. ASAIO J 2006;52(2):11A.
33. Ikeda S, Cunningham LA, Boggess D, Hobson CD, Sundberg JP, Naggert JK, et al. Aberrant actin cytoskeleton leads to accelerated proliferation of corneal epithelial cells in mice deficient for destrin (actin depolymerizing factor). Hum Mol Genet 2003;12(9):1028–36.
34. Hall A. Rho GTPases and the actin cytoskeleton. Science 1998;279:509–14. [PubMed: 9438836]
35. Huang S, Ingber DE. Cell tension, matrix mechanics, and cancer development. Cancer Cell 2005;8 (3):175–56. [PubMed: 16169461]
36. Wang N, Naruse K, Stamenovic D, Mijailovich JJFSM, Tolic′-Nørrelykke IM, Polte T, et al. Mechanical behavior in living cells consistent with the tensegrity model. Proc Natl Acad Sci USA 2001;98(14):7765–70. [PubMed: 11438729]

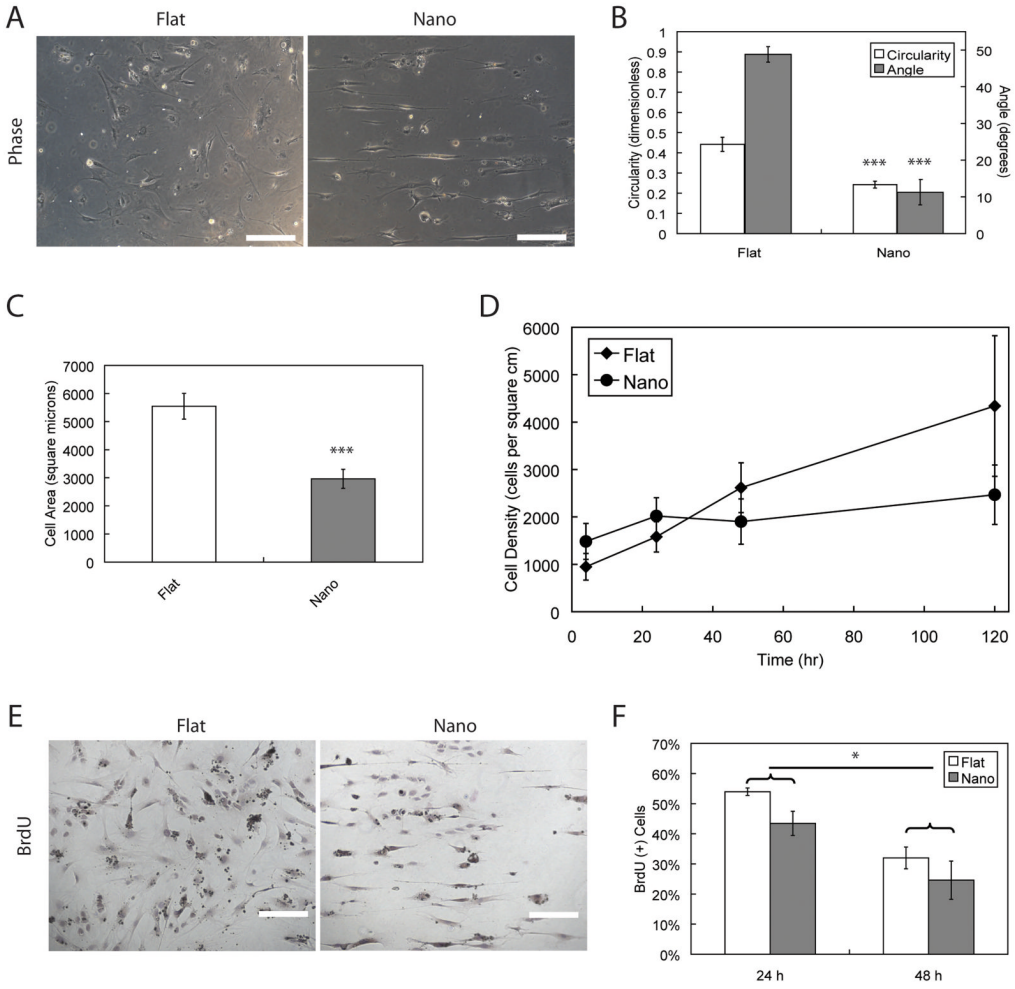

Figure 1. Morphological and proliferative response of hESCs to nanotopography

A) Phase images of hESCs cultured on flat and linear nanotopograhy PDMS substrates. B) Circularity and average angle of alignment (all graphical data is reported as mean +/− s.d.) were reduced on nanotopographic substrates when compared to flat substrate. C) Cells cultured on nanotopographic substrates exhibited lower projected cell areas as well as determined by t-test (*** $p < 0.001$). D) Cell growth kinetics showed that cells cultured on nanotopography had higher initial cell densities followed by stagnant proliferation. These kinetics were in contrast to those of cells grown on flat surfaces, which exhibited continued proliferation through 120 h. E) Representative color micrographs of BrdU assay revealed increased uptake of hESCs cultured on flat substrates compared to cells cultured on nanotopographic substrates after 24 h. F) BrdU uptake was reduced from 24 h to 48 h across both types of substrates. Statistical significance across 24 h and 48 h timepoints was determined by two-way ANOVA (* $p < 0.05$). Scale bars in all micrographs are 100 μm.

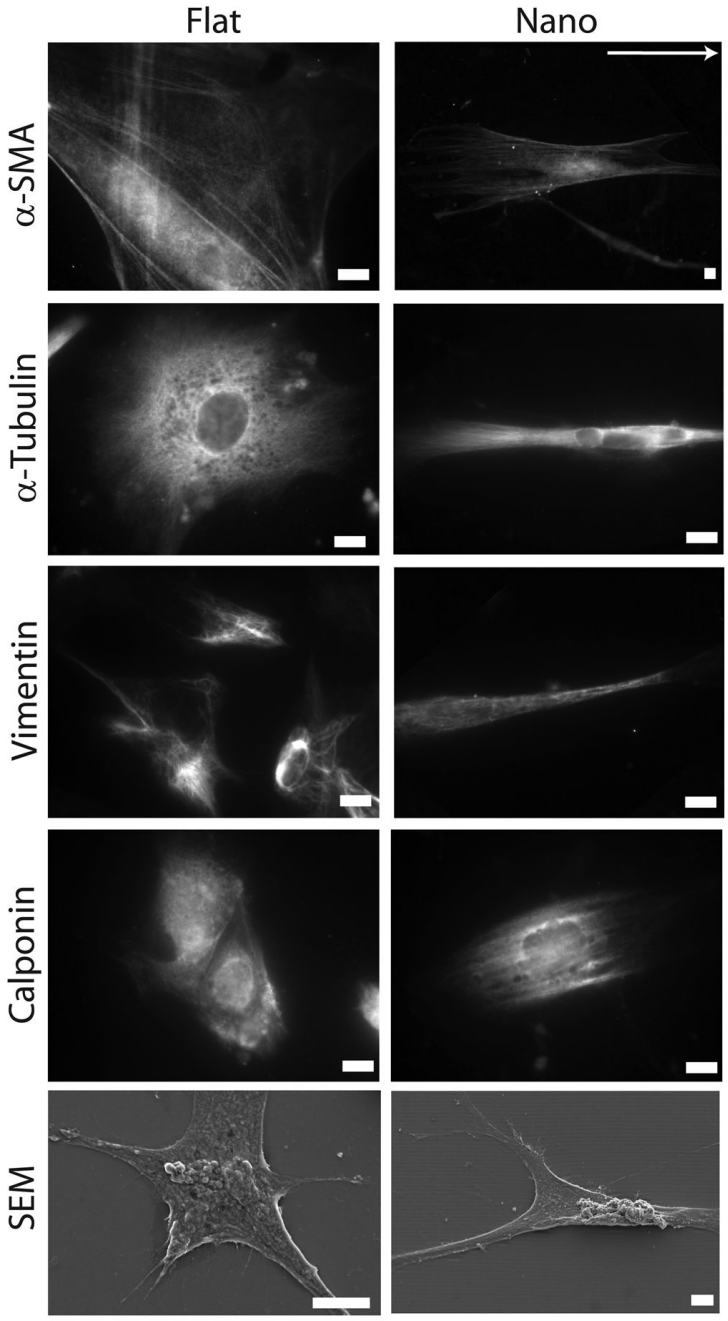

Figure 2. Nanotopography induces organization of cytoskeleton proteins

Human ESCs cultured on substrates with linear nanotopographic features responded to topography and exhibited organized cytoskeleton proteins including: α-SMA, α-tubulin, vimentin, and calponin. These morphological alterations were also confirmed through SEM micrographs. Direction of grid lines is indicated by white arrow. Scale bars are 10 μm.

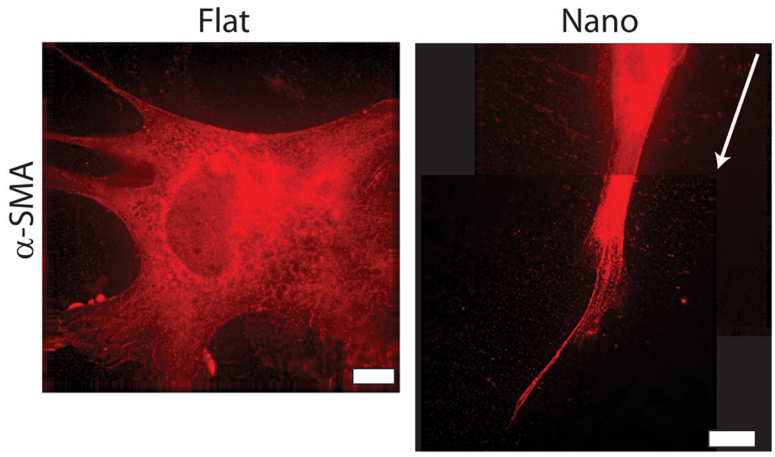

Figure 3. Deconvolution images of α-SMA in hESCs cultured on flat and nanotopographic substrates

Deconvolution images revealing α-SMA in hESCs cultured on flat substrates are globular without organization within the cytoskeleton (left panel). This observation lies in stark contrast to hESCs cultured on nanotopographic substrates (right panel) which exhibit organized aligned fibers in the direction of the nanotopography (right panel is a composite image of two micrographs). Direction of grid lines is indicated by white arrow. See online version for video of micrograph sections. Scale bars are 10 μm.

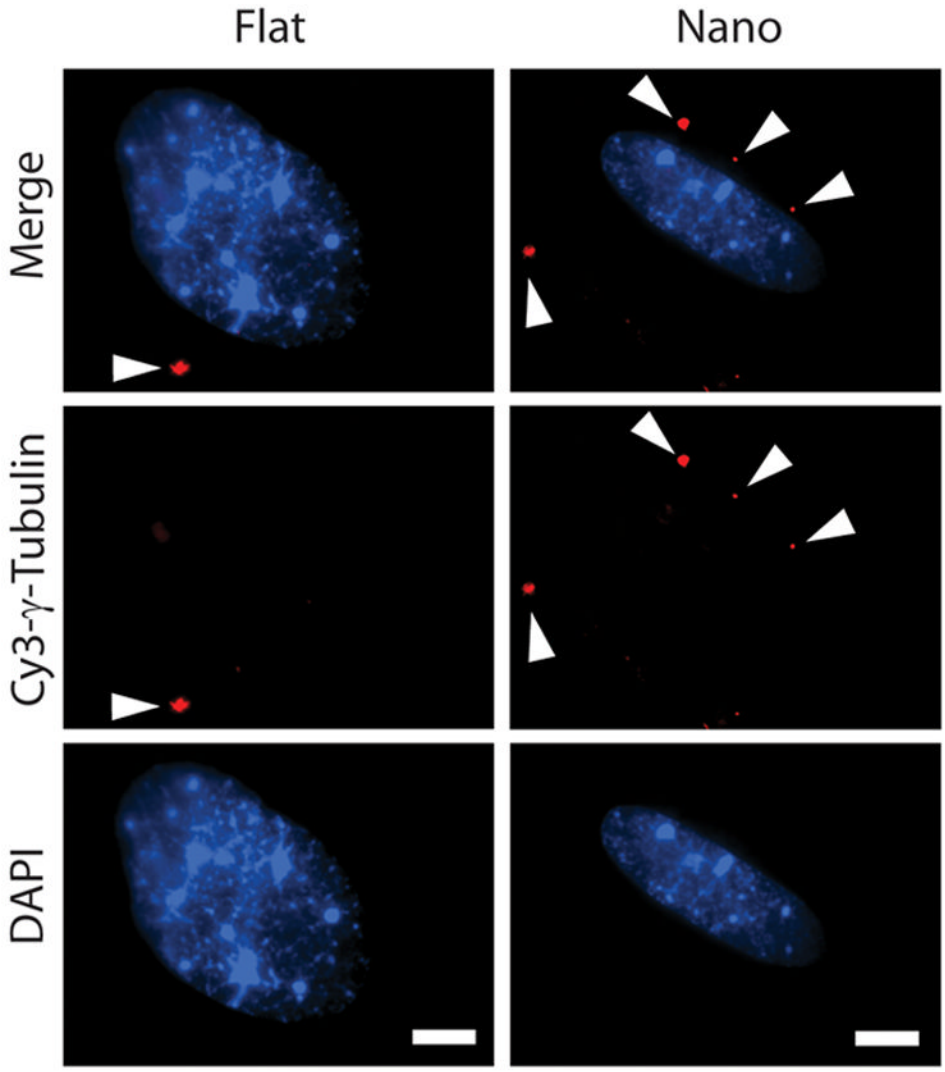

Figure 4. Nanotopography polarizes spatial distribution of gamma-tubulin complexes (GTCs) within hESCs

GTCs present in hESCs after 24 h of culture on flat substrates exhibit a random radial distribution with respect to the longitudinal axis of the nucleus when compared to cells cultured on nanotopographic substrates. Individual GTCs in each cell are indicated by white arrowheads. See Supplementary Fig 1 for additional information regarding the scoring of GTC alignment. Scale bars in all figures are 10 μm.

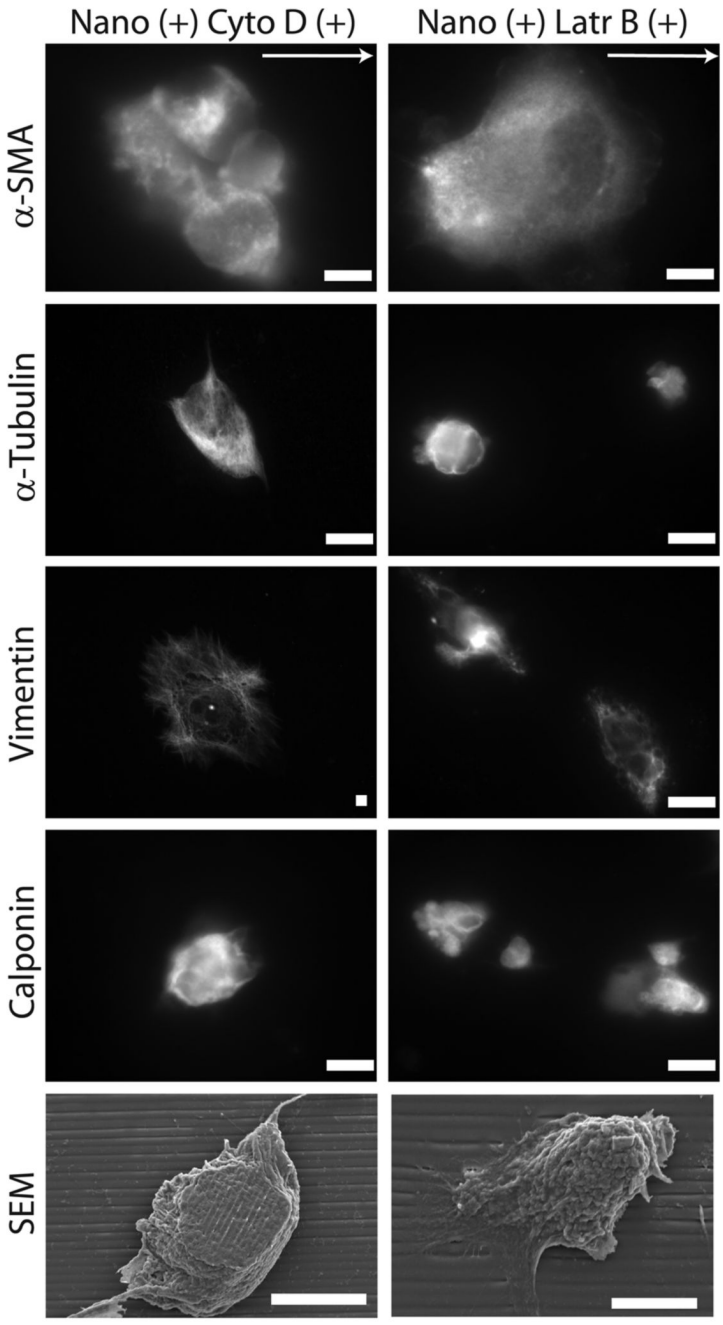

Figure 5. Actin-disrupting agents reduce nanotopography-mediated responses

Treatment of hESCs cultured on nanotopographic substrates, with cyto D, or latr B, two varieties of cytoskeleton disrupting agents, leads to a loss of cytoskeleton protein organization including α-SMA, vimentin, and α-tubulin. Culturing hESCs in the presence of ADAs also leads to a more rounded three-dimensional cell morphology. Scale bars are 10 μm.

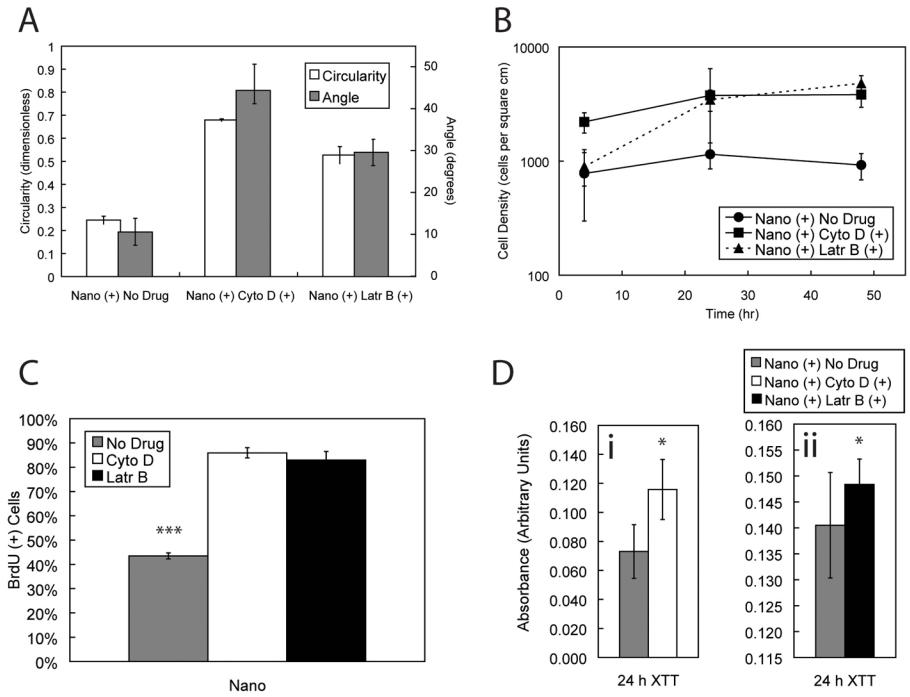

Figure 6. Actin disrupting agents reduce morphological, proliferative, and metabolic effects of nanotopography-induced contact guidance

A) Morphological characterization of cells cultured on nanotopographic substrates in the presence of cyto D and latr B resulted in increased circularity and a loss of bias of alignment angle as confirmed by one-way ANOVA (*** < p 0.001). B) Increased cell densities at time points 24 h, and 48 h as confirmed by two-way ANOVA (*** $p < 0.001$) in combination with increased BrdU uptake at 24 h as measured by one-way ANOVA (*** $p < 0.001$) (C) suggests that treatment with actin-disrupting agents leads to increased proliferation. D) Metabolic activity, as measured by XTT cleavage assay, increased for cells cultured with treatment of both cyto D (i) and latr B (ii) treatment at 24 h when compared to no drug as measured by t-tests (* $p < 0.05$, * $p < 0.05$ for cyto D and latr B, respectively).